

## SCARLET and Deep Space 1: Successfully Validating Advanced Solar Array Technology

John M. Stubstad  
Ballistic Missile Defense Organization  
Washington, DC

David Lehman and Paul M. Stella  
Jet Propulsion Laboratory  
Pasadena, CA

Ray Garza and David M. Murphy  
AEC-Able Engineering, Inc.  
Goleta, CA

Douglas M. Allen  
Schafer Corporation  
Dayton, OH

Technology (SCARLET). Although part of the advanced technology validation study, the array is also the power source for the spacecraft and its NASA Solar electric propulsion Technology Application Readiness (NSTAR) electric propulsion system. Sponsored by the Ballistic Missile Defense Organization (BMDO), the SCARLET concentrator solar array is the first application of a refractive lens concentrator designed for space applications.

As part of the DS1 validation process, the amount of diagnostics data acquired was more extensive than would be the norm for a more conventional solar array. These data include temperature measurements at numerous locations on the 2-wing, 4-panel per wing, solar array. For each panel, one 5-cell module in one of the circuit strings was wired so that a complete IV curve could be obtained. The data was used to verify sun pointing accuracy and array output performance. In addition, the spacecraft power load can be varied in a number of discrete steps, from a small fraction of the array total power capability, up to maximum power. For each of the power loads, array operating voltage could be measured along with the current output from each wing.

In-space measurements indicated that SCARLET performance was within one percent of predictions made from ground data prior to the flight.

### ABSTRACT

The Solar Concentrator Arrays with Refractive Linear Element Technology (SCARLET) system being used on the Deep Space 1 (DS1) spacecraft have been validated through successful performance in flight. DS1, launched in October 1998, will complete its primary mission in July 1999. SCARLET was developed by AEC-Able under BMDO sponsorship. DS1 was developed by JPL under NASA sponsorship. The SCARLET array uses linear, arched fresnel lens concentrators to focus sunlight onto narrow rows of multiple band gap solar cells to produce 2.5-kW of power. It is the first modular concentrator solar array ever used as prime power for a spacecraft. This paper describes the array technology, development process, array assembly and qualification, and flight operations. The array is providing power to the DS1 spacecraft and its NSTAR ion electric propulsion system. Results to date show that the pre-flight performance projections were within 1% of actual flight results, making SCARLET one of the highest performance solar arrays ever used in space.

### INTRODUCTION

On October 24, 1998, the first of the NASA New Millennium Spacecraft, Deep Space 1 (DS1), was successfully launched. The objectives for DS1 were to test advanced technologies that can reduce the cost or risk of future missions. One of these technologies is the Solar Concentrator Array with Refractive Linear Element

### BACKGROUND

SCARLET is a concentrator solar array for space applications which uses linear refractive Fresnel lenses to focus sunlight onto spaced rows of solar cells. For a given power level, the SCARLET optical system reduces the required solar cell area by approximately a factor of seven. The decreased cell area significantly reduces solar array cost and weight; especially for high radiation environments where a thick cell coverglass is required.

Development of the arched/domed Fresnel lens concentrator for space began in 1986 under a NASA Lewis Small Business Innovation Research (SBIR) contract with Entech, Inc. Early work focused on development of the mini-dome concentrator, a point-focus version of the concentrator element used by the current SCARLET design. Under NASA Lewis and BMDO funding, a number of prototype modules were built. These early units emphasized lens fabrication and lens/cell performance.

One of the most important concerns early in the program was the long-term stability of the concentrator lens material in the space environment. While

---

\* This paper is declared a work of the U.S. Government and is not subject to copyright protection in the United States

terrestrial-based testing provided significant information, the synergistic effects of the space environment made obtaining actual space flight data extremely important. The early mini-dome lens design used a self-supporting, space-qualified silicone (DC 93-500) with a multilayer coating to protect the silicone from the effects of atomic oxygen erosion and UV darkening. A number of passive Shuttle experiments (LDCE 4-5, EOIM-3, and Wakeshield) were conducted to support lens material characterization and evaluation. These early tests culminated with the fabrication of an active photovoltaic module for Photovoltaic Array Space Power Plus Diagnostics (PASP Plus) Experiment.

On August 3, 1994, the PASP Plus Experiment carried twelve different photovoltaic experiments into a high radiation geo-transfer orbit (GTO). The objective of the experiment was to test a variety of solar array/cell types under different environmental conditions. The highly elliptical orbit subjected the experiments to a proton-dominated, high-radiation environment, as well as wide variations in space plasma densities

In 1992, Entech began working on a line-focus version of its refractive concentrator concept for space. Based on the same general principles as the point-focus mini-dome concentrator, the linear concept offered two additional advantages over its predecessor: relaxation of precise array tracking requirements to only a single axis, and low-cost fabrication of the concentrator lens material. After verifying the performance of the linear concept through prototype testing, Entech teamed with AEC-Able to develop solar arrays using the line-focus lens. AEC-Able provided a unique capability in the design, fabrication, and testing of space structures and deployment mechanisms that turned the refractive line-focus concentrator concept into a viable commercial product.

In early 1995, an opportunity arose to fly SCARLET technology at the array level on the Multiple Experiments to Earth Orbit and Return (METEOR) spacecraft. The single-wing, six panel deployable array (four concentrator and two planar panels) demonstrated the first-generation implementation of SCARLET and first use of concentrator technology at the operational "array level". The array used the AEC-Able PUMA deployable structure, previously qualified as a planar array deployment system, with separate deployable concentrator lens panels to decrease the stowage volume of the array. The cell panels were populated with GaAs concentrator cell receivers supplied by Spectrolab, Inc. The time constraints associated with this opportunity required the project to go from concept definition to flight-qualified array in a period of six

months. Despite the schedule driven nature of this challenge, the hardware development and qualification program was a complete success. The array successfully completed acoustic, random vibration, thermal vacuum, deployed stiffness and strength, thermal ambient-environment deployment, and performance testing. Unfortunately, the loss of the Conestoga launch vehicle on October 23, 1995, prevented SCARLET-METEOR from obtaining useful flight data.

#### ARRAY DESIGN AND DEVELOPMENT

The design of the DS1 SCARLET array was an extension of the design knowledge accumulated from the SCARLET-METEOR array. The structural baseline was reassessed for the DS1 application to create a more elegant solution. The result was a simple cable-synchronized structure that deploys flat. The major advantages of this approach are that pointing is easier to analyze and control, and all lens frames are held securely between power panels during launch.

All the basic proven mechanisms, such as release assemblies, tiedown cup-cones, cable pullers, and hinges from the first SCARLET array were utilized again the DS1 SCARLET, but with redesigned components to minimize weight. Once the fundamental structural and component building blocks were in place, the task was to optimize their interaction. This involved a complex matrix of quantifiable variables entailing optical enhancement, thermal management, mass minimization, reliability augmentation, and part/assembly tolerance control traded against cost and less tangible criteria such as technical risk for DS1 and the role of the perceived risk in future marketability.

The details of the SCARLET technology have been described in a number of other papers, and will not be repeated here.<sup>1,2,3</sup> Likewise, the SCARLET program for the DS1 spacecraft has been described in previous papers.<sup>4,5</sup>

#### DESIGN OVERVIEW

The DS1 SCARLET array is composed of two wings. Each wing is made up of four panels plus a yoke assembly. The total length of each wing is 206-in. Each of the panels is 45-in x 63-in. Pictures of the completed array are shown in Figures 1, 2, and 3. Figure 1 shows one wing in the stowed configuration, Figure 2 shows it in mid deployment, and Figure 3 shows the array fully deployed. As described in the previous papers, a simple linkage mechanism is used to lift the concentrator lens frames to their proper height over the cells during the deployment.

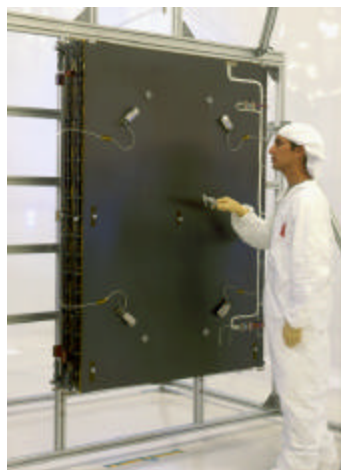


Figure 1: Stowed SCARLET Wing



Figure 2: SCARLET Wing in Mid-Deployment

The major performance parameters for the array are summarized in Table 1 below. The major components of the array were provided by:

- ? Entech, Fresnel lenses
- ? Composite Optics, composite structures
- ? Tecstar, multi-junction cells
- ? Hybrid Designs, cell module assemblies (CMAs)
- ? Moog/Schaeffer Magnetics, array drives
- ? AEC-Able, mechanisms

AEC-Able then assembled the array at their facility in Goleta, CA.



Figure 3: Deployed SCARLET Wing

| Parameter | Performance                                     |
|-----------|---|
| Power     | 2570 W at 1 AU                                  |
| Weight    | 29.3 kg, 44 W/kg Wing<br>60 W/kg at Panel Level |
| Stiffness | 0.42 Hz Deployed<br>92 Hz Stowed                |
| Strength  | >0.015 g Deployed                               |

Table 1: SCARLET Performance Parameters

SOLAR CELLS

The cell size used by SCARLET is 1.600-in. by 0.402-in active width (or about 1-cm x 4-cm). The small size and low total area per watt needed beneath the concentrator lens greatly lowers the cost and risk of utilizing emerging, high-performance cell technologies. For this reason, BMDO elected to take the industry lead and specify the procurement of an entirely multi-bandgap cell based solar array.

Tecstar was willing to participate, although their ability to perform as required was in question as the program began, because, in 1996, Tecstar, like Spectrolab, had not yet produced production quantities of GaInP<sub>2</sub>/GaAs/Ge dual junction cells. To mitigate risk, and to set performance criteria for the flight build, an engineering build quantity of 100 cells was procured.

Cells of a III-V design, termed “Cascade” by Tecstar had previously been qualified in the standard series of environments for space applications. The only modification required was gridline sizing for the high flux profiles of the concentrator. Through prototype evaluations it was determined the smallest gridline width that could be produced with reliable continuity was 9-mm. To achieve the optimum balance of sheet

resistance losses and gridline coverage the grid spacing was set at 200-mm.

The engineering evaluation result was very encouraging, with the average efficiency result coming in at 24.25%. The performance criteria for the flight build was set at 23.25% because of losses expected for glazing, as well as the uncertainties for a larger build.

During the flight production phase, Tecstar experienced a series of setbacks in producing the flight cells. The most persistent problem was shunting which reduced the performance of many of the cells to as low as 16% at 1 sun intensity. Fortunately, the high current injection level of the concentrator application overrides the fixed magnitude shunts and the performance at concentration is only slightly degraded. After intensive effort by Tecstar, and aided by the synergism of the early dual junction cell Mantech program, remarkable improvement in yield and performance were achieved. But delays in the schedule eventually forced the acceptance of cells with a minimum lot average, at concentration, of 22.7%.

#### RECEIVER MODULE

The cell receiver module consists of five series cells, each with bypass diodes, affixed to a circuit on a high thermal conductivity, carbon-carbon substrate. The modules were joined at overlapping redundant tabs using reflow solder to form 50 cell strings that generate 40 watts at an operating voltage of 92 volts at 1 Au.

Cells in the module are interconnected along both long edges. Given the long aspect ratio (4:1), the most probable crack direction would never leave a section of the cell isolated. Dual ohmics also provided balanced off-track performance and lower gridline resistance losses.

Cell interconnect reliability was greatly improved over standard CIC construction because 120 wires (in parallel per cell on both sides) connect the cell to the circuit board carrier. The automated ultrasonic wire bonder, stitching at a rate of three cells per minute, results in large cost savings by eliminating hand-labor.

Engineering modules underwent thermal cycling from -160°C to + 110°C for 100 cycles to assure a margin of compatibility with the single thermal cycle experienced on the DS1 mission at the start of its interplanetary mission. All modules experienced no visible degradation and comparison of pre and post IV curves under the X25 solar simulator at LeRC showed no measurable electrical degradation.

#### ARRAY ASSEMBLY AND QUALIFICATION

Assembling the SCARLET arrays included a number of steps. Three major subassemblies were assembled individually, followed by assembling these together. The subassemblies included the power panels (honeycomb panels with cell module assemblies), the lens frames, and the deployment mechanism (including the yoke, tie-downs, and release mechanisms).

#### POWER PANEL ASSEMBLY

The power panels start with delivery of the solar cells (with covers). The cells are then processed into cell module assemblies, consisting of five series connected cells on a single substrate. The substrate is a small composite element to provide rigidity and thermal conductivity. A Kapton circuit is attached to the substrate, then the cells are integrated onto the circuit. The integration into the circuit was originally accomplished by using a Nusal conductive silicon material to bond the cells to the circuit and also to provide the back cell contact. The top contacts are then made using a wire stitching process. This was accomplished using small Al wires.

Unfortunately, component testing revealed that both the top and bottom contacts were flawed. The conductive adhesive, which was rated up to 270°C, stopped conducting somewhere between 30° and 100°C. This was discovered after most of the cells had already been processed, so a procedure was developed to insert a bypass conductor to avoid damaging the cells. After testing a number of approaches, a "Solder Wire Insert Method" (SWIM) process was selected. The SWIM is a small, flattened section of flux core solder. Two of these were inserted under the edge of each cell, with the solder flowed by first preheating the cell module assembly and then applying a localized heat source at the SWIM using a hot air gun. The preheat was applied to reduce stress build-up when the solder cooled, after discovering microfractures in some cells during the process development.

The problem with the top contact was the Al wires used for the wire bonding were corroding. The Al apparently corroded due to the presence of chlorides on the cell metallization. The source of the chloride was never conclusively determined. However, the problem was resolved by replacing the Al wire bonds with Au wire bonds. This approach was verified using an 85/85 test (85% relative humidity at 85°C). However, applying the fix required removal of the modules from two panels that were already populated before the problem was discovered. Because of the dimensions of the wire-

stitching machine, the CMAs could not be repaired on the panels. They were removed and both the composite substrates and the surface of the honeycomb panels were cleaned.

The honeycomb panels were formed with Al cores and high conductivity composite facesheets. Ti inserts were used for high stress areas such as hinges and tie down points. During testing, it was discovered that very small cracks formed in the facesheets above the edge of the inserts when the panels were thermally cycled. Bonding doublers onto the facesheets in the areas of concern solved this problem. Mechanical testing verified this approach.

The CMAs were laid down on the honeycomb panels in rows at the focal lines of the concentrator lenses. The CMAs were wired together, with 10 modules forming a string, to provide 92V. Each panel has 9 strings, for a total of 450 cells per panel. Strings were joined into circuits at the edge of each panel, and fed into a harness that was wrapped around to the back side of the panel to join the harness from the other panels.

#### LENS FRAME ASSEMBLY

The individual SCARLET lenses are made of a specially designed Fresnel lens made from silicone bonded to a 3-mil glass superstrate. Each lens is 3.33-in wide by 8.38-in long to concentrate light onto a single 5 cell CMA. Figure 4 shows one section of the lens frame with a single lens over a 5-cell module. Assembling strips of composite material into a frame, with rectangular openings sized for the lenses, forms the lens frame. A linear lip was pinned onto the frame for the lenses to rest on, then the lenses were placed in the lips and bonded in place with a bead of silicone. No major problems were encountered in this process.

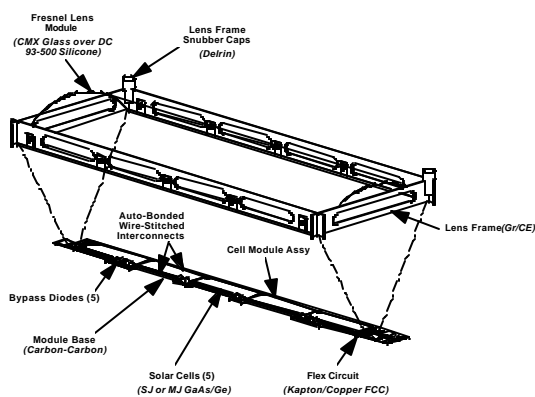


Figure 4: SCARLET Module Configuration

#### MECHANISM ASSEMBLY/ARRAY INTEGRATION

Mechanisms include the devices used to hold the wing in compression during launch, deploy the wings, and to point the wings in the alpha axis (the spacecraft turns to point in the beta axis).

The array is deployed using force from springs located at the hinge lines between the panels and at the root. Synchronization cables and dampers in the root mechanism are used to constrain the deployment and ensure that all the hinge lines open at the same rate. The lens frames were raised up over the power panels during deployment using a four bar mechanism on each panel plus hinge attachments between the first two and the last two lens frames.

Before deployment, the panels were held in the stowed position using four tie-down cables on each wing that pass through the panels and lens frames. Two release mechanisms on each wing are used to release the tie-down cables while the dampers and synchronization cables constrain the deployment to limit the forces on the structural panels.

Finally, a solar array drive mechanism was attached to the root of the wing to enable rotating the array to point it at the sun.

The only significant design related issue in this area that arose during assembly was a question about what would happen if the array was deployed with one edge hot and one edge cold. This condition would occur if the sun was shining on one edge. To verify that this would not be a problem, the synchronization cables were modified to use small diameter composite tubes for most of the cable length. A composite with a zero coefficient of thermal expansion was selected to eliminate the hot edge/cold edge force differentials.

#### QUALIFICATION TESTING

Wing qualification testing was initiated once assembly of each wing was completed. Due to financial constraints, no spare hardware was fabricated and a protoflight test approach on the flight hardware was used. The levels for the protoflight testing were defined by the DS1 Component Verification Specification (CVS).<sup>6</sup>

Figure 5 shows the individual tests that were included in the program as well as the order that the tests were performed. Following each of the major tests (thermal cycle, acoustic, random vibration), the wing was deployed and inspected to verify that no critical damage occurred during the test. Before and after the full testing sequence, a full electrical functional test was performed on the wing to verify that the power level and

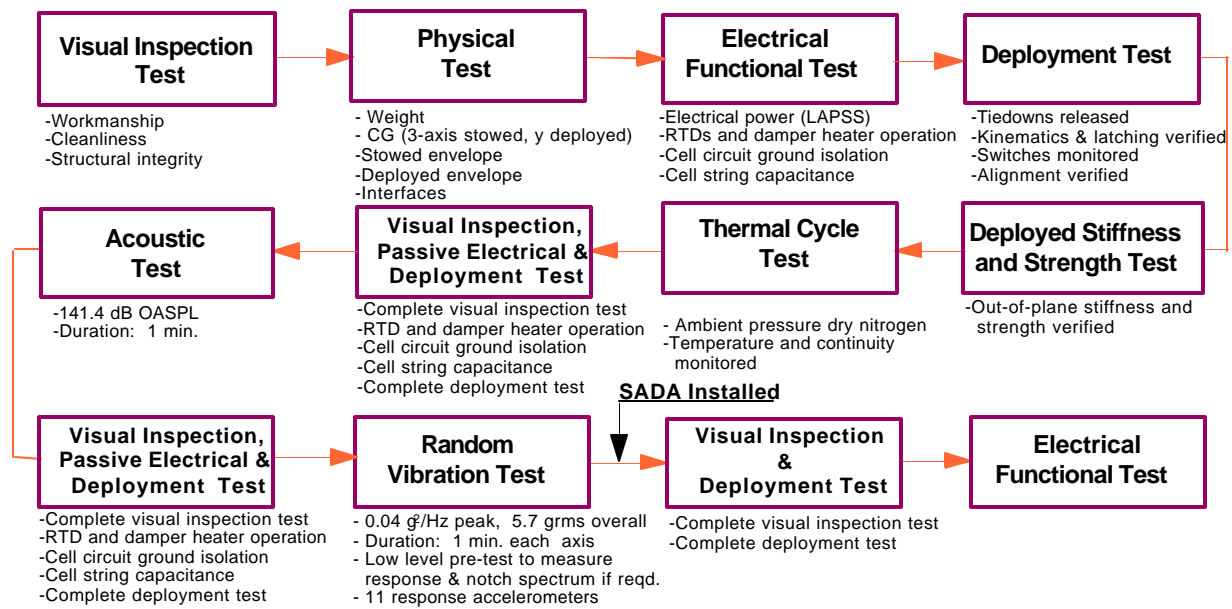


Figure 5: Protoflight Test Sequence

electrical functionality of the wing was not degraded by the exposure to the test environments.

#### DEPLOYMENT TESTS

As part of the initial deployment tests, the array was deployed at thermal extremes, including a 10°C margin, based on modeling of the possible conditions in space at the time of deployment. The array was successfully deployed at -66°C, 30°C, and at ambient temperature.

An attempt was also made to test the array under a thermal gradient condition to simulate the case discussed previously of the sun shining directly on one edge of the wing. The wing was first cooled in a thermal chamber. Quartz heaters were then used to heat the bottom edge of the wing. The goal was to reach -60°C on the top edge with the bottom edge heated to +10°C. However, this thermal gradient could not be attained due to the limitations of the test equipment. Consequently, applying extra tension to the top synchronization cables was used to simulate the anticipated effect of the gradient. All of the deployment tests were completed successfully.

#### THERMAL CYCLE TEST

Thermal cycling was not a major issue for the DS1 mission because after the spacecraft leaves the earth's shadow following launch, it is in the sun for the rest of the mission. However, the CVS required a limited number of thermal cycles to ensure that the initial cycle from ambient (launch) to cold (umbra) to hot (in the sun) would not be a problem.

The wings were cycled three times between -123°C and +113°C. The hot and cold temperatures were held for 5 minutes during each cycle. The temperatures were determined by mission analysis of the hottest and coldest possible conditions, plus margin. The tests were conducted in a dry nitrogen environment. Prior to array assembly, all of the flight array components had also gone through at least three thermal cycles.

Following the test, the arrays showed no measurable power reduction and no structural damage. Nearly 4% of the glass concentrator lens superstrates developed small cracks during the testing. However, the shape of the lens was maintained because the curved shape was formed in a zero stress state. The silicone adhesive also helped to maintain the configuration of the lens. No deformation or optical degradation was observed in the cracked lenses. All of the cracked lenses subsequently survived the acoustic and random vibration environments. Thus, the program decided not to replace the cracked lenses.

#### ACOUSTIC TEST

The wings were exposed to acoustic environments between 105 and 135-dB over a frequency range of 30- to 10000-Hz during a 1-minute test. The arrays experienced no measurable power reduction or structural damage due to the test. As with the thermal cycle test, a small number of concentrator lens glass superstrates were cracked during the test, less than 2% of superstrates in this case. Again, there was no deformation or optical degradation and all of these

lenses subsequently survived the random vibration test. No other problems were observed during this test.

**RANDOM VIBRATION TEST**

The wings were random vibration tested in all three axes to the levels shown in Table 2. The test duration was one minute in each axis. As with the previous protoflight test, the arrays experienced no measurable power reduction or structural damage due to the test. Again, a small number of concentrator lens glass superstrates were cracked during the test; in this case, less than 1% of superstrates. Again, there was no deformation or optical degradation.

| Frequency (Hz) | PSD (g <sup>2</sup> /Hz) |
|----------------|--------------------------|
| 20             | 0.0016                   |
| 50             | 0.04                     |
| 500            | 0.04                     |

Table 2: Random Vibration Test Levels

Following random vibration, one of the status indicator switches on the tie-down mechanism was found to be open. Its normal state is closed. A three dimensional x-ray showed that a ceramic nub had broken inside the micro-switch. It was determined that shock from the tie-down release broke the switch insulator bond-line. Subsequent vibration caused the component to come loose. It was determined that a pre-existing crack in the ceramic insulator led to this failure.

To prevent this from occurring during flight, a foam bumper was added to the tie-down mechanism release arm. Additionally, a procedure was added to screen the switch's ceramic insulator under 930X magnification before switch assembly.

**POWER MEASUREMENT**

The power was measured using a Large Area Pulse Solar Simulator (LAPSS). Due to the concentrator lenses, the light must be collimated perpendicular to the wing for the power to be measured. This required that wing power be measured one string at a time. The configuration of the strings results in an area of 17.3-cm across by 110-cm wide for each string. Testing showed that the light from the LAPSS was sufficiently collimated over this area.

All of the measurements performed as expected during these tests. Figure 6 shows the results of testing a string with and without the concentrator lenses. The string  $I_{sc}$  for a long series string was consistent with the measured average lens concentration ratio of 7.14. The

string  $V_{oc}$  boost of 8% was consistent with individual module results. The string  $P_{max}$  increased by 4% more than expected (increased fill factor). This was determined to be due to the presence of shunts in some of the cells. Under concentration, the cells generate more current, so the shunts become less significant.

**INTEGRATION AND FLIGHT**

Due to the need to protect the arrays prior to launch and the mass of the array protective covers, it was decided to ship the SCARLET wings to the launch site in separate shipping containers and integrate the wings to the spacecraft there. The array was shipped with the spacecraft from JPL, in the separate containers. Upon arrival, they were checked both visually and electrically, using a complex impedance measurement and continuity check. The wings were then mechanically and electrically integrated into the spacecraft prior to the spin balance procedure. Again, the arrays were checked and certified to be ready for flight.

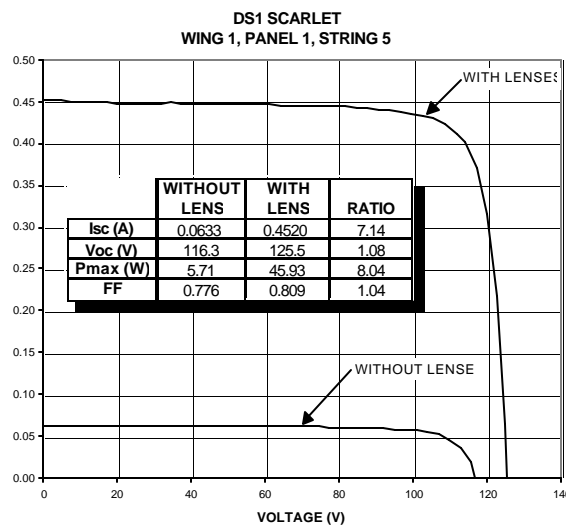


Figure 6: SCARLET String I-V Curves

**DEPLOYMENT**

The first activity required from the SCARLET system in space, deployment, occurred 1 hour after launch after power was autonomously commanded to be applied to the Solar Array Tiedown Mechanisms (SATMs). At that point, the spacecraft was in eclipse on the far side of the Earth. Telemetry was recorded at 5second intervals. Forty minutes later, when the real time link was reestablished at JPL, it was evident that the array had deployed; the indicator switch states were all in agreement and power was being produced.

POINTING

The proper alignment of a concentrator system is critical. System performance is dependent on all elements (cells, modules, lens frames, panels, hinges, yoke, etc.) being assembled accurately, deployed reliably, and being resistant to thermal distortion. Numerous industry efforts to build concentrator systems have failed at various stages prior to launch due to the inherent design and manufacturing difficulties. The industry has had success of late with low concentration ratios, for example the planned Hughes 702 reflective trough concentrator at 2X. SCARLET is the first system on-orbit to provide significant concentration benefits. The Fresnel optics provide an advantage in tolerance to shape error that reflective systems lack.

A typical data set shows the performance of the total system begins to falloff just beyond 1 degree, as expected. When the data for each module is plotted a parabolic curve fit can be used to estimate whether the alignment is centered or skewed. The population of data shows scattering due to spacecraft drift. However, the best fit curves form a fair assessment of the focal line offset on each cell module. When the offsets are compared against the design specifications, as in Figure 5, the success of the system in achieving far better alignment than required is clearly evident.

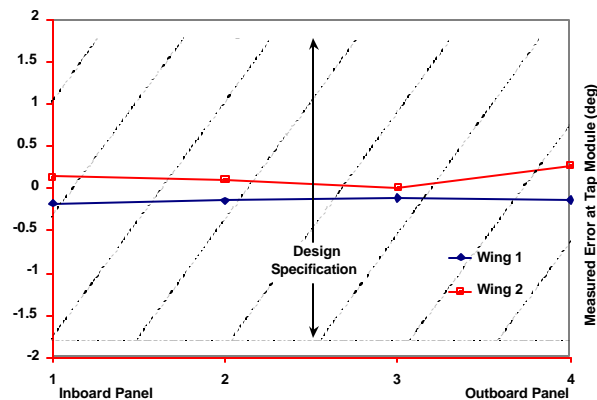


Figure 7: Pointing Validation Summary

TEMPERATURE

The first critical validation of the power model is the operating temperature of the array. Each wing was equipped with four RTDs on the inboard panel and four more on the outboard panel

On the 37<sup>th</sup> day of the mission the ion engine was, for the first time, commanded to thrust at increasing increments up to maximum power. The data available just on all the front RTDs (nearest the cells) for array

power levels between zero and near full power are plotted in Figure 8.

The model prediction curve is also plotted for comparison. The general agreement is excellent. Several observations about the data can be made. First, the agreement is fairly precise, on average, near maximum power for the RTDs nearest the cells. Second, the flight data of the other RTDs show the temperature gradients spreading across and through the panel were slightly larger than forecast by the model.

POWER

The validation of power production relies on two sequences: SIVPerf and SPeak. SIVPerf measures the full IV curve of a single module within a string of 10 modules on each panel, for a total of eight module level curves. SPeak produces a partial IV curve for each wing, as a byproduct of a sequence intended to optimize thrusting. The SIVPerf results will be discussed first.

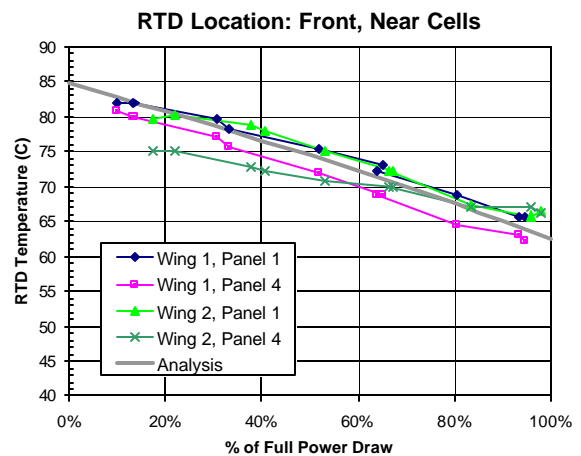


Figure 8. Steady State Temperature vs. Power Draw

SIVPerf

This sequence was intended to be run on the earliest day possible after launch using all 8 tap circuits and the 10 RTD temperature sensors to verify initial performance prior to on-orbit calibration. Thereafter, it was to be run nominally every month as a minimum to validate performance versus AU, temperature, and environmental degradations. The first SIVPerf was run on mission day 7, October 31, 1998. Examination of the first data set was not encouraging. The fill factors on several curves were low. It was noted that on average, the tap modules were producing about 4% less power than expected based on the pre-flight LAPSS tests. The preliminary results suggested that, for mission planning purposes, it would be best to use the worse case array

power predictions until full array IV curves could be obtained during the week of 9 November 1998. As a consequence of delays due to various spacecraft anomalies, obtaining peak power results from the first full power thrusting was postponed until November 30<sup>th</sup>. When these data were analyzed it was found the early extrapolation from the tap module results were too conservative. The wings were actually producing at or above the nominal power prediction. It is not clear why some of the tap modules have shown low fill factors while overall the array is performing well. Only one other SIVPerf sequence has been run, so there is limited data available.

SIVPerf runs have been limited because during the second running of the sequence, on mission day 18 (November 11<sup>th</sup>), an anomaly was observed: the heaters for the paraffin array release devices were powered. Due to the interruption of the sequence the data point for  $V_{oc}$  is missing on the 7<sup>th</sup> module and the 8<sup>th</sup> was not recorded at all. It had not been noticed until later that on the first run, 9 November, the last data point on the 8<sup>th</sup> module was dropped. At that time no spacecraft anomalies were observed.

The SIVPerf sequence provides certain types of data the SPeak test cannot: namely, data to the left of peak power on the IV curve. Short circuit current is of interest as it validates the lens optical efficiency and functions as a monitor for UV or radiation darkening, or outgassing contamination. A comparison of the  $I_{sc}$  values for the modules on days 7 and 18 shows no change when corrected for insolation changes due to heliocentric distance. This indicates that there is no significant darkening taking place during the initial weeks in space. However, contamination of the lenses from spacecraft or array outgassing may have already occurred. Resistance to long term UV and/or radiation darkening cannot be deduced from this limited data, but initial indications are that these effects are small, as expected.

The predicted  $I_{sc}$  was slightly higher (within 1%) than the flight measurements, once corrected for temperature, initial degradation, and time-based degradation.

The open circuit voltage is of interest because it can be used as another method, besides the RTD results measurements, to validate the thermal model. Open circuit voltage is reduced linearly with increasing temperature, keeping the intensity constant, in accordance with the voltage coefficient, which was modeled as  $-5.0 \text{ mV}/^\circ\text{C}$  per cell. In Table 3, the average values for wings 1 and 2 are scaled by the average ratio of the tap circuit  $V_{oc}$  to the array  $V_{oc}$  from LAPSS testing, then compared to the predicted values.

| Average Module $V_{oc}$ , volts | String Equivalent $V_{oc}$ , volts | Predicted Array $V_{oc}$ , volts | Ratio Flight to Predict |
|---------------------------------|------------------------------------|----------------------------------|-------------------------|
| 11.55 (Day 7)                   | 114.83                             | 104.8                            | 1.10                    |
| 11.51 (Day 18)                  | 114.38                             | 105.0                            | 1.09                    |

Table 3: Flight Tap Module  $V_{oc}$  vs. Predicted  $V_{oc}$

The flight results were much higher than expected. The prediction based on LAPSS results were corrected for only three effects: peak power operating temperature, temperature rise when under low power draw, and thermal coefficient for voltage. To match the model to the flight voltage, the cell operating temperature would have to have been  $40^\circ\text{C}$  lower, or the thermal coefficient would have to be 55% lower. Neither option is considered reasonable. The array level voltage varies over the mission as the heliocentric distance varies. This gives a rich data source for voltage study that should be explored before any conclusions are drawn from the aberrantly high module level voltages.

Given the intermittent thrusting over the first 120 days of the mission, 75% of the time the array power draw was only about 15% of capacity. Thus the voltage is near the point of interest: open circuit. A few of the available data points were tabulated and a trendline was fitted as shown in Figure 9. This issue is described in detail along with a discussion of future planned work to understand the cause of the higher voltages a recent paper.<sup>7</sup>

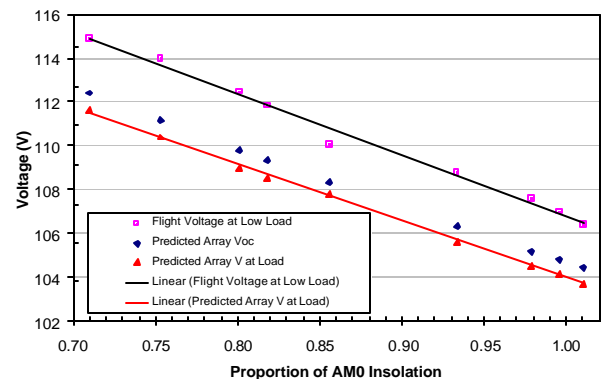


Figure 9: Array Voltage at Low Load vs. Flux

The entire IV curve can be obtained during the SIVPerf sequence. The curves for the first module are shown in Figure 10.

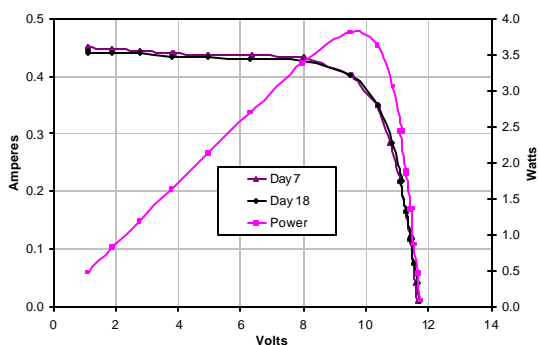


Figure 10: Tap Module Performance - Wing 1, Panel 1

For this particular module, the power output has not fallen although the incident light has dropped 1%. For three others the fill factors were lower than expected and one decreased significantly between days 7 and 18. The obvious question is: If one of eight modules is losing performance, then what is happening at the array level? This question was examined by the SPeak sequence.

SPeak

The first, and to date only, SPeak sequence, on mission day 90, began by incrementally increasing the ion engine power level, stopping at two intermediate points between nominal bus loads and maximum power. This was done to allow intermediate power level data to be recorded and to let the array cool to near the full power operating temperature before moving to the full power load voltage. The last setting was chosen to be about 100-W in excess of the expected maximum power. The battery was relied upon to supply the differential power. The EPS was designed with the capability to utilize the batteries as a buffer to allow maximum thruster output without collapse. If the proper low voltage set point and thruster level are selected, this algorithm allows the solar array to operate at peak power and provides data for array level performance. The SPeak sequence adjusts the set point voltage through a range yielding more data along the performance curve near peak power. The SPeak software will step down the thrust level if the battery discharge exceeds a predetermined level.

During this test run, the load voltage set point was intentionally stepped lower at 0.3-V increments to obtain detailed data. When the array peak power was approached, the increments of voltage resulted in negligible array power output change. Plotting the wing currents against voltage rather than time, yields the more familiar "IV" curve. A detail of the data near the knee is shown in Figure 11.

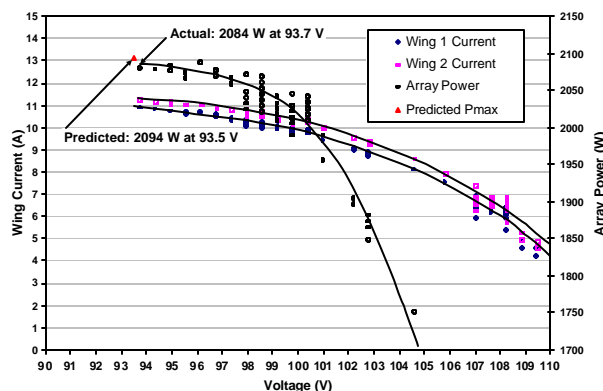


Figure 11: SPeak Data, Array Output at 1.1185 AU

The power output has leveled off to 2084-W, as the voltage was reduced to the last recorded value of 93.7V. Flight values from the best fit curve are compared to model predictions in Table 4.

The excellent agreement between the forecast and the flight results - for the best data set available to date on the mission - is the clearest validation of the SCARLET technology.

| Value               | V <sub>mp</sub> (volts) | P <sub>max</sub> (watts) |
|---------------------|-------------------------|--------------------------|
| Prediction (P)      | 93.5                    | 2094                     |
| Flight Results (FR) | 93.7                    | 2084                     |
| FR/P Ratio          | 1.003                   | 0.995                    |

Table 4: SPeak Results Comparison

CONCLUSION

The performance of SCARLET on Deep Space 1 substantially validated all aspects of the novel structural platform, Fresnel optics, multi-junction cell module performance, and electrical design. The major features of safe stowage through launch, deployment, and sun acquisition were clearly demonstrated on the first day of the mission. Stability of the array system, in particular, the ability to maintain the relatively tight pointing, has been verified over more than eight months. The array performance has continued to achieve design specifications without imposing any special requirements on the spacecraft.

A number of detail parameters, such as open circuit voltage, have shown minor deviation from the design predictions. Causes have been discussed, some of which include errors in the data itself, but no array problem is suspected. Continuing acquisition of data throughout the mission is expected to better help identify the cause of these discrepancies. SPeak, for example, has only been performed once. However, it is

important to note that none of the discrepancies impact the array capability to provide the required mission power over the mission lifetime. To a certain extent they reflect the unusually high level of array diagnostics that are available.

In fact, given the range of variables in the cells (2 and 3 junction), coverglass (IR reflecting and non-IR reflecting), and lens coating (with anti-reflecting and without); and the present limitations of the data quantity and quality; it is a testimony to the soundness of the SCARLET design and manufacture that the array performance has met the mission needs and that the power output has so closely tracked the nominal forecast.

#### ACKNOWLEDGEMENTS

The research described in this paper was performed under the sponsorship of the Ballistic Missile Defense Organization and the National Aeronautics and Space Administration. The success of DS1 and the SCARLET technology reflects the efforts of the many engineers and technicians who produced a working system out of many novel technologies. Patience and commitment to problem solving of the team members at ABLE, BMDO, and JPL were all critical to the achievement.

#### REFERENCES

1. D.M. Allen, P.A. Jones, D.M. Murphy, and M.F. Piszczor, "The SCARLET Light Concentrating Solar Array," *Conference Record of the Twenty Fifth IEEE Photovoltaic Specialists Conference*, IEEE, New York, NY (1996).
2. P. A. Jones, D. M. Murphy, T. J. Harvey, D. M. Allen, L. H. Caveny, M. F. Piszczor, "SCARLET: A High-Payoff, Near-Term Concentrator Solar Array," *ICSSC*, Paper 96-1021, AIAA, Washington DC (1996).
3. B. Spence, "SCARLET Solar Array System Study for High Power GEO Spacecraft," *Proceedings of the 15th Space Photovoltaic Research and Technology Conference (SPRAT)*, NASA Lewis Research Center, Cleveland, OH (1997).
4. A.B. Chmielewski, A. Das, C. Cassapakis, D. Allen, J. Sercel, Piszczor, P.A. Jones, D.M. Barnett, T. Reddy, "The New Millennium Program Power Technology," *Proceedings of the 31st Intersociety Energy Conversion Engineering Conference*, IEEE, New York, NY (1996).
5. D. M. Murphy and D.M. Allen, "SCARLET Development, Fabrication, and Testing for the Deep Space 1 Spacecraft," *Proceedings of the 32nd Intersociety Energy Conversion Engineering Conference*, AIChE, New York, NY (1997).
6. W.T. Hall, et. al., Component And Spacecraft Verification Specification, New Millennium Deep Space Mission 1, JPL document DS1 No. 6446-361, Jet Propulsion Laboratory, Pasadena, CA (1996).
7. P.M. Stella, D.G. Nieraeth, D.M. Murphy, M.I. Eskenazi, and J. Stubstad, "Validation of the SCARLET Advanced Array on DS1," *Proceedings of the 34th Intersociety Energy Conversion Engineering Conference*, SAE, Warrendale, PA (1999).